

Gold Tablets: Gold Nanoparticles Encapsulated into Dextran Tablets and Their pH-Responsive Behavior as an Easy-to-Use Platform for Multipurpose Applications

Zubi Sadiq, Seyed Hamid Safiabadi Tali, and Sana Jahanshahi-Anbuhi*

Cite This: *ACS Omega* 2022, 7, 11177–11189

Read Online

ACCESS |



Metrics & More

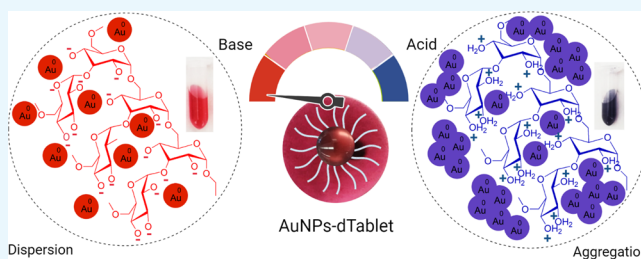


Article Recommendations



Supporting Information

ABSTRACT: Many applications using gold nanoparticles (AuNPs) require (i) their functionalization with a biopolymer to increase their stability and (ii) their transformation into an easy-to-handle material, which provide them with specific properties. In this research, a portable tablet platform is presented based on dextran-encapsulated gold nanoparticles (AuNPs-dTab) by a ligand exchange reaction between citrate-capped gold nanoparticles (AuNPs-Cit) and dextran. These newly fabricated tablets were characterized utilizing ultraviolet–visible spectroscopy (UV–vis), Fourier transform infrared spectroscopy–attenuated total reflectance (FTIR–ATR), transmission electron microscopy (TEM), dynamic light scattering (DLS), X-ray diffraction spectroscopy (XRD), differential scanning calorimetry (DSC), and atomic force microscopy (AFM) techniques. The results showed that dextran-capped gold nanoparticles in a tablet platform (AuNPs-dTab) were well-dispersed and highly stable for at least a year at room temperature. In addition to particle and surface characterization of AuNPs-dTab, the tablet morphology in terms of thickness, diameter, density, and opacity was also measured using 6 and 10% dextran with 2, 4 and 8 nM AuNPs-Cit. We further investigated the pH-responsive behavior of AuNPs-dTab in the presence and absence of sodium chloride. Results showed that neutral and alkaline environments were suitable to render AuNPs dispersed in a tablet, while an acidic condition controls the aggregation rate of AuNPs as confirmed by concentration-dependent aggregation phenomena. Besides the easy fabrication, these tablets were portable and low-cost (approx. 1.22 CAD per 100 tablets of a 100 μ L solution of dextran-capped gold nanoparticles (AuNPs-dSol)). The biocompatible nature of dextran along with the acidic medium trigger nature of AuNPs makes our proposed tablet a potential candidate for cancer therapy due to the acidic surrounding of tumor tissues as compared to normal cells. Also, our proposed tablet approach paves the way for the fabrication of portable and easy-to-use optical sensors based on the AuNPs embedded in a natural polymeric architecture that would serve as a colorimetric recognition indicator for detecting analytes of interest.



INTRODUCTION

Gold nanoparticles (AuNPs) have diverse applications in the area of heterogeneous catalysis,¹ food sciences,² biomedical engineering,^{3–5} drug delivery,^{6,7} biosensing^{8–11} bioimaging,¹² and many more. These nanoparticles have shown remarkable chemical, biological, optical, thermal, and electronic characteristics. Several chemical, biological, and physical approaches have been reported for the synthesis of these nanometallic particles under mild conditions.^{13–15} Their ease of preparation, variable surface chemistry, and nano size variation make AuNPs suitable candidates for a range of applications such as food packaging, water purification, batteries, nanoceramics, and electronics.^{16–19} One of the aspects is the surface plasmon resonance phenomenon, which is a fundamental principle of many colorimetric sensing applications. This unique feature can be tuned sharply based on the surrounding functionality and stabilization forces around nanogold as well as their interparticle distance and morphology. Usually, citrate-capped gold nanoparticles are electrostatically stabilized and are very

sensitive to ionic strength. Alternatively, if particles are sterically stable instead of electrostatic forces, e.g., in the case of polymer bound gold nanoparticles, these particles are less prone to aggregation and offer extra stability in high salt concentrations.²⁰ That is why these particles have been engineered with different capping agents depending upon the required properties according to the target of interest.

In connection with this, extensive research has been conducted over many decades to investigate the potential applications of AuNPs. Various studies have been performed to explore the colorimetric role of AuNPs in the detection of toxins in food,²¹ in hazardous substances in the environment,²²

Received: December 31, 2021

Accepted: March 7, 2022

Published: March 22, 2022



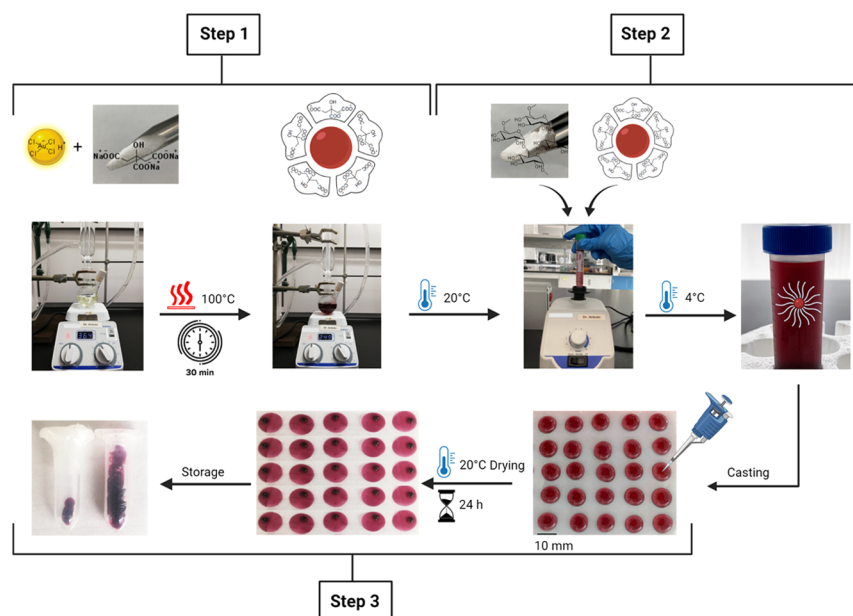


Figure 1. Representation of AuNPs-dTab formation stepwise. In step 1, citrate-capped gold nanoparticles (AuNPs-Cit) were synthesized by boiling chloroauric acid with sodium citrate for 30 min. In step 2, dextran powder was added to the cooled solution of AuNPs-Cit, mixed well using a vortex to get a homogenized dextran-capped gold nanoparticle (AuNPs-dSol) solution, and stored in a fridge. In step 3, AuNPs-dTabs were casted by a pipetting technique followed by air drying for 24 h at room temperature and finally stored in airtight plastic vials. The tablets were portable and low-cost (approx. 1.22 CAD per 100 tablets of 100 μL).

as well as in forensics and diverse biomedical applications. For example, aptamer wrapped AuNPs have been reported for the detection of T2-toxin in wheat and corn,²³ aflatoxins in milk,^{24,25} and antibiotics in many food and environmental samples.²⁶ Recently, Zha *et al.* reported a dual-modal immunosensor based on biotin-labeled IgG-modified AuNPs for the detection of chloroacetamide herbicides.²⁷ Also, sodium malonate capped AuNPs were reported for the detection of barium ions in gunshot residues as a potential application in forensic sciences.²⁸

AuNPs are also famous due to their distinct position in disease diagnostics and nanomedicine due to their compatibility with biomolecules.^{29,30} Under controlled conditions, these nanoparticles are well-dispersed, stable in media, and red in color. However, a fluctuation in temperature and pH dramatically changes the electrostatic stabilization of gold nanoparticles and favors the aggregation of particles corresponding to a blue color. That is why their thermoresponsive and pH-responsive behavior is important to mention whenever their role in sensing and biomedical applications is investigated.³¹ Most of the chemical linkages are sensitive to an acidic environment such as the hydrolysis of acetal, ketal, ester, amide, imine, hydrazone, and oxime.^{32,33} Gold nanoparticles as drug-loaded acid-degradable nanocarriers can be administered to the body through intravenous injection, and hence, this acid-induced degradation is important in living systems because it allows the release of encapsulated therapeutics in a controlled/enhanced fashion.³³ In this connection, dextran-stabilized AuNPs are of particular interest because these particles utilize the functional properties of both entities to maximize their benefits.

Dextran is a natural biocompatible and biodegradable homopolysaccharide of glucose that has historical significance in pharmaceutical and medical applications.³⁴ This polymer also has a strong ability to surround AuNPs due to the $-\text{OH}$ and $-\text{COR}$ groups in its chains that stabilize nanoparticles

through steric as well as electrostatic forces.²⁰ These hydroxyl groups in polymeric chain have been oxidized to carbonyl functionality when dextran is primarily used as a reducing agent during the synthesis of AuNPs. Utilizing this concept, Wang *et al.* reported the colorimetric detection of dihydralazine sulfate in uric samples based on hydrazone chemistry between the aldehydic group of dextran and the hydrazine moiety of the analyte.³⁵ In another report, Davidović *et al.* detected cysteine colorimetrically by replacing dextran from the nanoparticle as the thiol group interacts more strongly with metallic particles compared to ketone and aldehyde groups of dextran.³⁶ On the other hand, when dextran is used exclusively as a surface coating material around AuNPs, it may require harsh reaction conditions to break its polymeric steric stabilization. It is important to point out that the long-term stability is a prerequisite for any application of colloids.

Due to these outstanding characteristics, various formats of dextran-encapsulated AuNPs have been developed including colloidal solutions, gold nanocomposites/hydrogels³⁷ as well as powder³⁸ with applications in drug delivery,²⁹ cell imaging,³⁹ wound healing,⁴⁰ and microbial susceptibility.⁴¹ Nonetheless, dextran-capped AuNP solutions gradually aggregate to form bigger particles due to the sedimentation phenomenon of AuNPs in colloidal systems after some time. On the other hand, the storage and transportation of AuNP solutions are not always convenient. In fact, it was observed that several samples of the synthesized dextran functionalized AuNP solutions stored at normal conditions were randomly attacked by fungi.³⁸ In the case of powdered/gel samples, there is a serious issue of quantitative measurement of AuNPs-dSol powder/gels for a specific test every time, and hence, these samples are not suitable for direct applications and require extensive calibration procedures.

Keeping these issues in mind and in addition to our ongoing efforts to fabricate portable sensors for environmental monitoring and provide easy-to-use platforms,^{42–44} we have

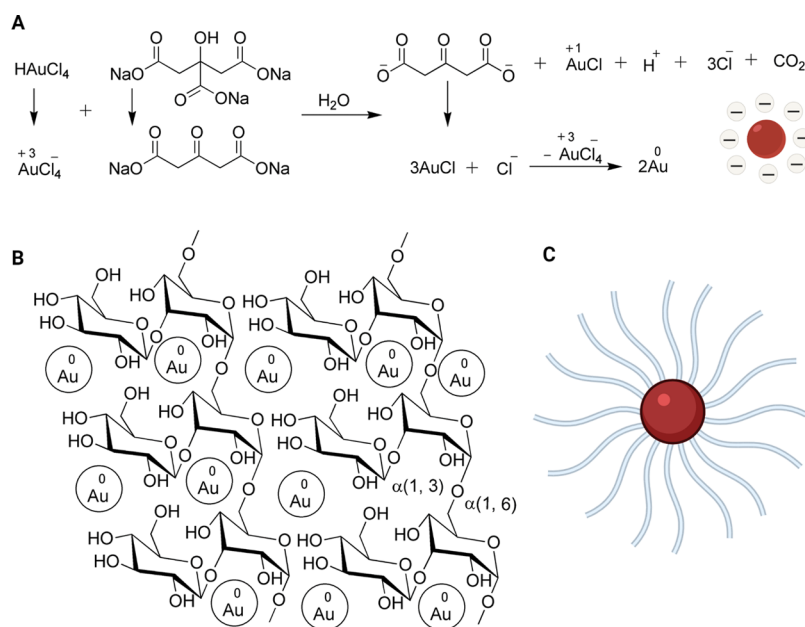


Figure 2. Chemical outline of the synthesized gold nanoparticles. (A) Stepwise chemical reactions involved in Turkevich protocols for the synthesis of AuNPs-Cit that are electrostatically stabilized as shown by the charged red circle in the right corner. (B) Proposed structural representation of AuNPs-dSol where nanoparticles are embedded in the dextran biopolymer. (C) Electrosteric stabilization of dextran around nanoparticles in AuNPs-dSol.

developed a dextran-based AuNPs tablet (AuNPs-dTab) as a simple and ultrastable platform for multipurpose applications. These tablets can be prepared in different concentrations of colloidal gold with a variable amount of dextran; hence, a premeasured and calibrated/optimized amount of dextran-capped AuNPs can be stored in the form of solid tablets. These preloaded tablets with the right mass of reagent will lower the user interventions and eliminate the need for a weighing balance, pipettes, and other equipment. Our approach is an easy substitute of the solution phase of AuNPs-dSol without compromising the stability and efficiency of nanoparticles.

The tablets were obtained in three easy steps without involving any laborious workup as mentioned in Figure 1. In this study, after optimization of the fabrication technique with various concentrations of dextran, we spectroscopically characterized the tablets using UV-vis, FTIR, DLS, TEM, XRD, DSC, and AFM techniques. Next, we demonstrated the outstanding stability of AuNPs-dTab under ambient conditions as well as at high salt concentrations. These tablets showed pH tolerance in the alkaline condition, while the tablets were highly responsive at a lower pH as the aggregation of nanogold in acidic pH range is an important feature of colorimetric sensors. Being oxygen impermeable, these tablets are highly stable against oxidative stress in addition to their thermal stability. Our proposed fabricated AuNPs-dTabs are stable for 9 months and even longer as no stability issue is recorded till the preparation of this manuscript. The morphology of these tablets was also analyzed in terms of thickness, diameter, density, and opacity. In short, this simple, easy-to-store, and easy-to-carry tablet opens new avenues in biosensing and biotechnology research due to being user-friendly and low-cost.

RESULTS AND DISCUSSION

We prepared the dextran-encapsulated gold nanoparticles-based tablets (AuNPs-dTabs) by mixing the colloidal

suspension of citrate-stabilized AuNP with dextran powder. These tablets were fully characterized by UV-vis, FTIR, TEM, DLS, XRD, DSC, and AFM techniques. Their pH-responsive behavior toward neutral, acidic, and basic environments was investigated to show the effect of a range of pH values toward the stabilization of AuNPs. Moreover, the AuNPs-dTab morphology has been explained in terms of its diameter, thickness, opacity, and density.

AuNPs-Cit were achieved by conventional Turkevich protocols using a direct method where the bottom-up approach is followed to reduce the Au^{+3} ions with a reducing agent as mentioned in Figure 2A. In this method, nontoxic citrate ions electrostatically stabilize spherical gold colloids. Different Au^{+3} complexes with citrates are exhibited in a solution at a given time.⁴⁵ In a typical direct procedure, a solution of sodium citrate is added to a refluxed and stirred solution of hydrogen tetrachloroaurate at a fixed ratio. Here, citrate acts as a surfactant as well as reducing agent, and the pH of the reaction solution gradually changes from acidic to neutral. The color of the gold colloidal suspension depends on the size and shape of AuNPs, which will affect the wavelength of light that is scattered and absorbed; thus, the evolution of color with time is a qualitative measure of the rate of particle formation.⁴⁵ This approach is considerably reproducible as Kettemann *et al.* have presented monodispersed particles with a reproducibility of ± 0.1 nm.⁴⁵

In a simplified bioconjugation procedure, AuNPs-Cit were turned into AuNPs-dSol by a ligand exchange reaction under mild reaction conditions. The proposed chemical structure of AuNPs embedded in a dextran matrix is presented in Figure 2B. Dextran, being a strong ligand as compared to citrate ions, can easily surround gold nanoparticles without any adjustment of solution pH and hence acts as an efficient capping agent as shown in Figure 2C. However, the direct one-pot synthesis of AuNPs-dSol is time consuming and requires harsh reaction conditions such as an extremely basic pH (12) and a prolonged

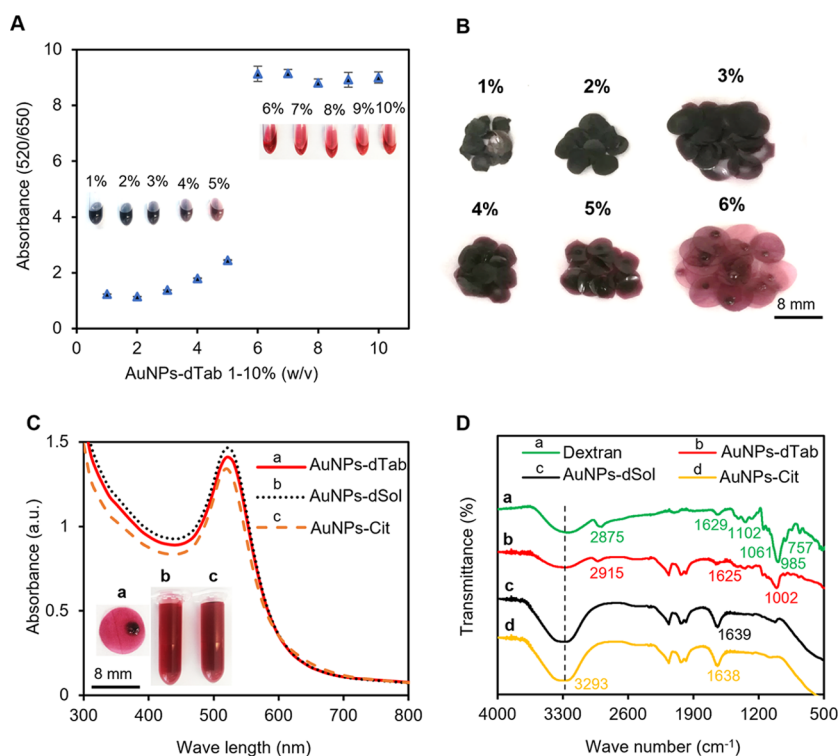


Figure 3. A pictorial and spectroscopic characterization of AuNPs-dTab. (A) Screening at A520/650 of different concentrations (1–10% (w/v)) of AuNPs-dTab dissolved in 200 μL of water using a UV–vis spectrophotometer. (B) Different concentrations of AuNPs-dTab (1–6% (w/v)). (C) UV–vis spectra of AuNPs-dTab, AuNPs-dSol, and AuNPs-Cit. (D) FTIR spectra of pure dextran, AuNPs-dTab, AuNPs-dSol, and AuNPs-Cit.

reaction time of 12 h.⁶ Similarly, Tang *et al.* reported the hydroxide-assisted synthesis of AuNPs-dSol utilizing a 1 M sodium hydroxide solution that is strongly basic.⁴⁶ It is also well-known that, upon variation of pH, the hydrophilic–hydrophobic balance of some polymers can be disturbed by the change in the ionization state of the weak acid or base groups. In this context, special attention has been given to explore the pH-responsive behavior of AuNPs-dTab.

Optimization of the Dextran Concentration. The easiest approach to coat plasmonic AuNPs with dextran is to homogeneously mix the dextran powder with the appropriate volume of colloidal citrated-capped AuNPs. Over time, dextran, being a strong stabilizing and capping agent, removes the citrate ligands around AuNPs by a ligand exchange reaction and surrounds the nanoparticles very tightly. For this purpose, the concentration of the polysaccharide solution in weight by volume was used to cast the tablets where 10% (w/v) dextran in AuNPs solution (AuNPs-dSol) was prepared as a stock that was subsequently used in the preparation of dilution series ranging from 1 to 9%. From this study, it was found that 6% (w/v) AuNPs-dTab was the optimum concentration that maintained all the nanoparticles in the fully dispersed stage as shown in Figure 3A. So, this concentration was selected for further investigations as a lower amount of dextran in 1–3% (w/v) solution was not sufficient to stabilize AuNPs till 24 h. That is why blue tablets were formed that showed the aggregated phase of AuNPs and guided us to enhance the stabilizing agent. AuNPs-dTabs from 4 and 5% solution were dark purple and purple red, respectively, which indicated the need for a little more dextran to completely stabilize the AuNPs as shown in Figure 3B. Finally, the 6% AuNPs-dSol solution produced red tablets in which AuNPs remained completely dispersed and stable for an extended period of time

(see section **Stability and Storage of AuNPs-dTabs**) because, in general, polysaccharides such as dextran, chitosan, hyaluronan, and alginate with oxygen-rich structures in hydroxyl and ether groups lead to tight binding to nanoparticles via a steric and electrostatic interaction.³⁸ Results from 7–10% AuNPs-dTabs were similar to 6%; however, a higher concentration of dextran was avoided to enable breaking the stabilization under mild conditions.

AuNPs-dTab was characterized using spectroscopic and microscopic techniques as well as DLS measurements, and the results were compared with AuNPs-Cit and AuNPs-dSol solution whenever required. In the case of optical analysis under UV–vis, maximum absorption spectra appeared at 520 nm as mentioned in Figure 3C, where the inset displays an image of deep red suspensions of AuNPs-Cit and AuNPs-dSol solution along with AuNPs-dTab. The surface plasmon resonance (SPR) band is produced through collective oscillations of free conduction electrons of AuNPs. Essentially, the extinction spectra of all three nanomaterial samples were the same. The maximum absorption band appeared at a wavelength of 520 nm for all three samples, which is a characteristic of 13 nm AuNPs. The concentration of the AuNP-dSol colloidal solution was 8.1 nmol L^{-1} by means of Lambert–Beer’s law, wherein the value of ϵ used was $2.7 \times 10^8 \text{ L mol}^{-1} \text{ cm}^{-1}$.⁴² This result demonstrated that the particles were fully dispersed, and their size was almost in the same range with AuNPs-Cit and AuNPs-dSol without any contamination as a change in size or dispersibility would change the place of the absorption maxima.⁴⁷ It is a proven fact that by increasing the particle size of nanogold, the absorption maxima move toward a higher wavelength, resulting in a bathochromic (red) shift. Moreover, the peak intensity of all samples was similar, showing that the encapsulation of gold

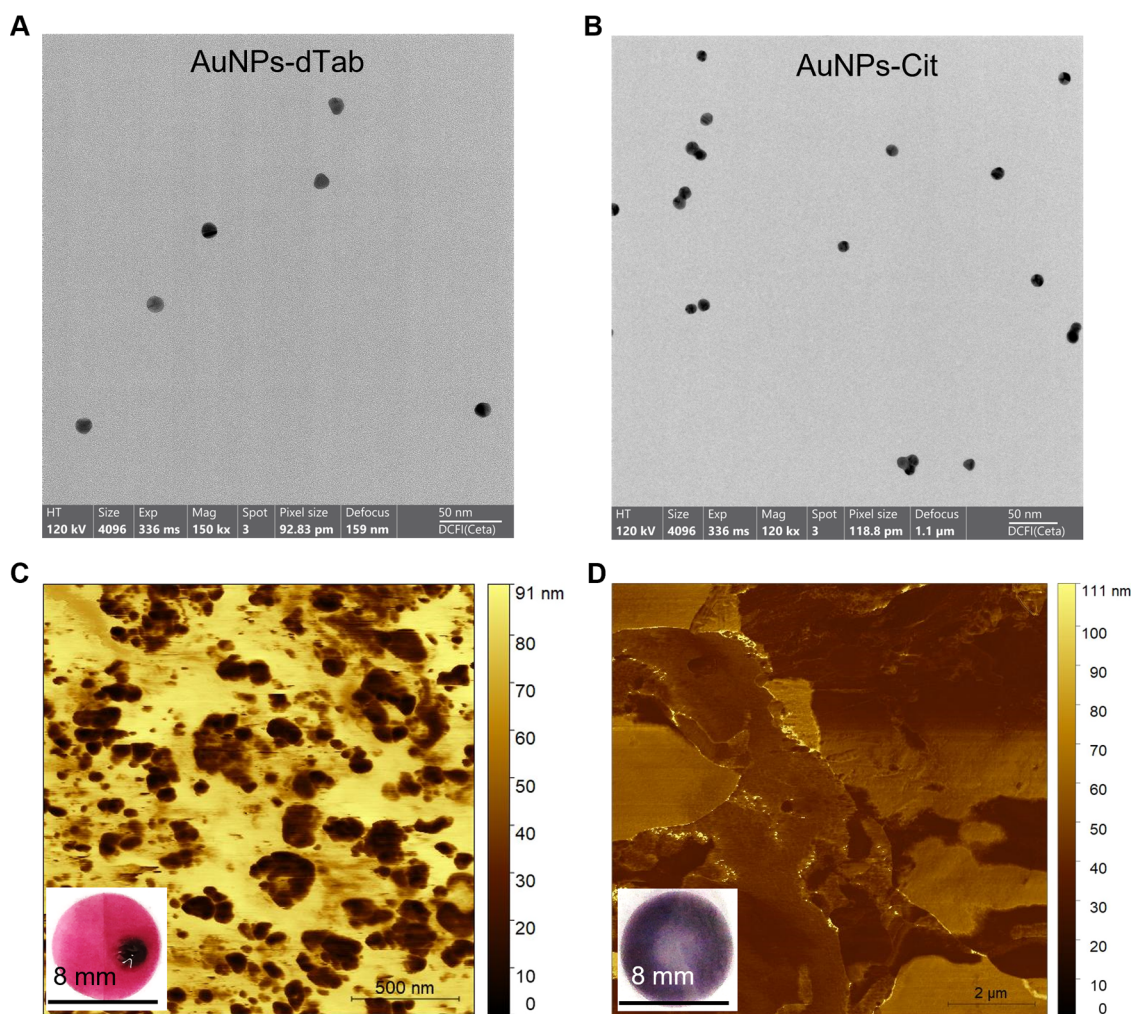


Figure 4. Images representing the morphological analysis of AuNPs-dTab in terms of particle and tablet material. (A) TEM image of AuNPs-dTab showing the size and spherical shape of particles. (B) TEM image of AuNPs-Cit indicating the size and shape of particles. (C) The phase trace AFM image of AuNPs-dTab showing the dispersed state of nanoparticles in an "active" red tablet. (D) Phase trace of AuNPs-dTab showing the aggregated state of nanoparticles in a "dead" purple tablet.

nanoparticles in the form of a tablet did not interfere with the performance of the particles, and these particles were equally effective and stable as in the case of the solution. Thus, our tablet platform is suitable for all those applications where the solution phase of AuNP-dextran is used while eliminating any complexity in handling and transportation.

Interactions of dextran with AuNPs were identified using Attenuated total reflectance Fourier transform infrared (ATR-FTIR) spectra. Figure 3D demonstrates the results for the four samples of pure dextran, AuNPs-dTab, AuNPs-dSol, and AuNPs-Cit pure dextran powder were compared with AuNPs-dTab and AuNPs-dSol spectra. The spectrum plotted in green represents the spectrum of dextran, whereas the curve plotted in red, black, and yellow represents the spectrum of AuNPs-dTab, AuNPs-dSol solution, and AuNPs-Cit solution, respectively. Apparently, the AuNPs-dTab spectrum is similar to the AuNPs-dSol spectrum with a major difference of peak intensity at 3293 cm^{-1} that is due to the symmetric stretching vibration mode of the OH group of water.⁴⁶ This peak is less wide in a tablet as compared to a similar broad peak in the AuNPs-dSol solution. Moreover, the intensity of this peak is comparable to the intensity of the similar peak for powder dextran, so it also confirms the dehydrated state of our tablet

due to the evaporation of solvent molecules. The peak at 2875 cm^{-1} is assigned to $-\text{CH}$ group stretching vibrations of dextran, while it has shifted to 2915 cm^{-1} in AuNPs-dTab. The bands at 1102 , 1061 , and 985 cm^{-1} correspond to the stretching vibrations of C–O bonds, the alcoholic hydroxyl (C–OH), and α -glycosidic bonds (C–O–C) in dextran, respectively.⁴⁶ Similar bands but with less intensity were observed in the AuNPs-Tab spectrum, so these changes indicated the strong interactions of dextran with AuNPs. An absorption band appeared at 1639 cm^{-1} due to the C=O stretching vibration mode present in the spectrum of AuNPs-dSol and AuNPs-Cit, which suggested the involvement of the C=O group in the formation of AuNPs.⁶ The peak intensity was similar for both liquid samples, while it was less intense in the case of solid samples AuNPs-Tab and dextran powder. This fact might be due to the strong H-bonding of the C=O group with water in a solution phase. Also, a common pattern was observed near 2160 and 1977 cm^{-1} for all the samples except pure dextran, which indicated the similar nature of the materials. Hence, FTIR measurements showed that dextran molecules were involved in the fabrication of AuNPs-dTab.

In conclusion, AuNPs-dTABS were fabricated with 6% (w/v) solution of AuNPs-dSol for further investigations as this

concentration was the optimum amount of dextran that kept the nanoparticles stable for an extended period. It was also clear that the particle size remained unchanged when we transformed the AuNPs-dSol liquid phase to the solid AuNPs-dTab.

Dextran-Encapsulated AuNPs-Tablets (AuNPs-dTabs). Tablets from AuNPs-dSol solution 6% (w/v) were casted to measure surface characterization and record the stability test. Tablet formation is considered complete only if the tablet leaves the hydrophobic surface of the plastic sheet freely and has a constant weight. Tablets were casted by pipetting out a fixed volume of the solution instead of the drop squeezing method to maintain a similar amount of captured nanoparticles in each tablet. Mostly wine-red round-shaped tablets were produced, but a quasi-spherical shape was also observed due to the difference in the drying environment as shown in Figure S1. We dispensed a variety of droplets ranging from 100 to 500 μL of the solution and collected small and big tablets depending on the volume. By this strategy, premeasured quantities of reagents can be easily stored inside the tablets. Our tablet-based encapsulation approach is more beneficial than the powdered AuNPs-dSol³⁸ due to the storing of a known amount of substances, which are ready to use.

The amount of dextran has a direct influence on the size of nanoparticles as by increasing the dextran quantity, the size of the AuNPs decreased with a few exceptions.^{38,46} In our study, dextran was used in the ligand exchange reaction to replace the citrate ions and was not involved in the reduction of hydrogen tetrachloroaurate, so the size of the nanogold might remain the same in any concentration of dextran above 5%. The particle size and shape of AuNPs-dTab and AuNPs-Cit were estimated through their TEM images as shown in Figure 4A,B, respectively. The average particle size for AuNPs-dTab and AuNPs-Cit was found to be 11.74 ± 1.39 and 11.53 ± 1.48 nm, respectively. Gold nanoparticles remained spherical in shape and uniform irrespective of the nature of the capping agent.

DLS measurement was also recorded for AuNPs-dTab, AuNPs-dSol, and AuNPs-Cit solutions in triplicate. The hydrodynamic diameter of the AuNPs-Cit solution was found to be 14.38 ± 1.39 nm with a polydispersity index (PDI) of 37.80%, whereas this diameter was changed to a much higher value of 127.17 ± 5.81 nm with a PDI of 24.43% for the AuNPs-dSol solution, which indicated the successful surface modification of particles from citrate to dextran by the ligand exchange method. However, when particles were embedded into the dextran matrix as the tablet platform, these particles became much bigger as shown by the average hydrodynamic diameter of AuNPs-dTab by DLS of 304.12 ± 16.43 nm with a PDI of 17.33%, although the particle's diameter was 11.70 nm by TEM analysis, which confirmed that the particle diameter in a tablet did not change because the diameter of the particle along with the surrounding capping agent is considered in the case of DLS measurement, whereas TEM analysis records the diameter of the nanoparticle alone. Blue tablets indicated the presence of aggregation between particles, which makes them bigger as confirmed by their hydrodynamic diameter of 686.5 ± 136.13 nm with a PDI of 17.3% by DLS studies.

Additionally, we have investigated various physical characteristics such as the thickness, diameter, weight, density, and opacity of the tablets using 6 and 10% dextran with 2, 4, and 8 nM AuNP concentrations to better understand the effects of

these parameters on the tablets. The maximum thickness was 0.71 ± 0.10 mm for the 10% dextran tablets with 4 nM AuNPs. The maximum diameter recorded for the tablets was 7.64 ± 0.17 mm for the 6% dextran tablets with 2 nM AuNPs. The maximum weight observed was 4.3 ± 0.3 mg for the 10% tablets with 8 nM AuNPs. The maximum density was 0.247 ± 0.0039 g/cm³ for the 6% dextran tablets with 8 nM AuNPs. The maximum opacity was 4.009 ± 0.107 for the 6% dextran tablets with 8 nM AuNPs. For the detailed procedure and results, refer to Figure S2A,B. Overall, the increase in the concentration of dextran significantly increased the thickness, diameter, and weight of the tablets, while it decreased the opacity and had no significant effect on the density.

To analyze the AuNPs with their surrounding environment in the solid state of the tablets, high-resolution surface images of AuNPs-dTab were taken using AFM scanning probe microscopy. AuNPs were embedded into the dextran matrix as dispersed particles when the tablet is red in color and as aggregated particles in the case of a blue tablet as shown in Figure 4DC,, respectively. The phase trace image in Figure 4C shows that the mean height of the AuNPs was 10–30 nm, indicating that the AuNPs are well-dispersed throughout the exopolysaccharide substance. The biggest gold particle in the given image has a diameter 90.60 nm. For the 2D and 3D height profile of AuNPs-dTab as surface roughness and texture description, see Figure S3. These particles have a round shape as also supported by the TEM image. It could be explained by the fact that free alcoholic hydroxyl groups of dextran are able to stabilize AuNPs by the interaction between the surface Au atoms of AuNPs and oxygen atoms of dextran. Importantly, a high density of hydroxyl functionality in dextran could lead to extensive inter- and intramolecular hydrogen bonding, favoring the stability and dispersion of AuNPs.⁴⁸ Hence, AFM results showed that AuNPs were distributed mainly on the surface of polysaccharide and offered strong interaction in a tablet when particles are dispersed. In the case of the blue tablet, particles were aggregated and considered as "nonresponsive" toward SPR phenomena. The crystallinity and thermal stability of AuNPs-dTab were recorded using XRD and DSC analysis, and results are reported in Figure S4.

Stability and Storage of AuNPs-dTabs. AuNPs-dTabs were kept at room temperature and in a fridge in an open and air-tight sealed packing for different durations before being tested for their stability. Generally, AuNPs are very stable when surrounded by a stabilizing agent under controlled conditions. Stabilizers are either charged species like citrate ions that offer ionic stabilization or a neutral surface bound matrix like dextran that offers steric and electrostatic stabilization. Dextran has a hyperbranched structure that has oxygen-rich functionalities like hydroxyl and ether groups, which lead to a tight binding with nanogold clusters via electrosteric interactions.⁴⁹ Electrostatic particles are kinetically stabilized, while steric force generates thermodynamic stabilization.⁵⁰

AuNPs-dTabs were dried for 24 h and then stored at different conditions. The AuNPs-dSol solution was used as the control to compare and measure the stability of nanoparticles encapsulated in the tablets. UV–vis absorption at 520 nm for the four samples of the AuNPs-dTab and AuNPs-dSol solution at 20 °C (referred to as room temperature or RT) and the AuNPs-dTab and AuNPs-dSol solution at 4 °C (referred to as fridge or FR) showed almost similar intensities for up to 3 weeks as depicted in Figure S5. However, there was a gradual decrease in stability for the AuNPs-dSol solution placed at

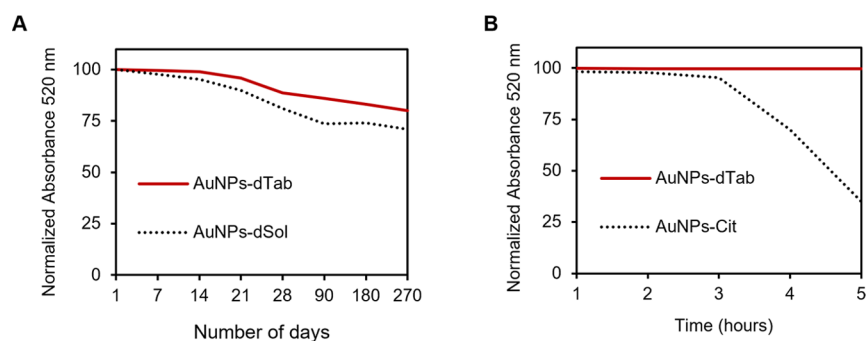


Figure 5. A comparative study of the stability profile of AuNPs-dTab with AuNPs-dSol and AuNPs-Cit. (A) AuNPs-dTab showing a higher stability as compared to AuNPs-dSol at room temperature (20 °C) till 9 months. (B) AuNPs-dTab stability remained unaffected till 5 h, while the AuNPs-Cit solution was stable only for 3 h followed by a sudden decrease in stability that was approximately 30 and 65% in 4 and 5 h, respectively, under operating environmental conditions of continuous light exposure and humidity at room temperature.

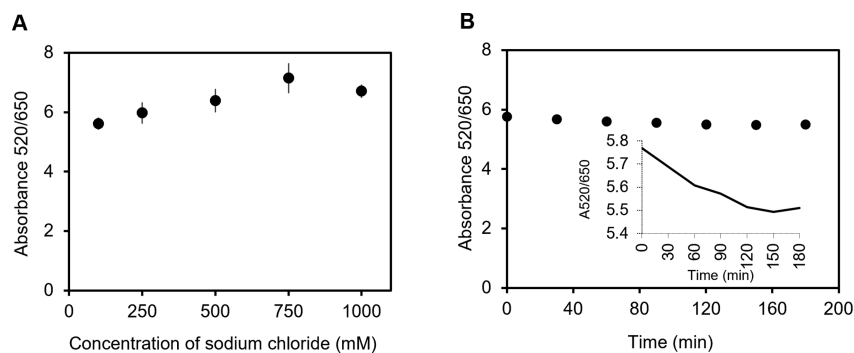


Figure 6. Effect of the ionic solution on AuNPs-dTab 6% (w/v). (A) Screening of different concentrations of sodium chloride with AuNPs-dTab in a 1:1 ratio. (B) Kinetic study of AuNPs-dTab with 100 mM NaCl solution till 3 h where the inset highlights the change during this period for the 520/650 absorbance ratio value in the range of 5.4 to 5.8. This figure indicated that the rate of aggregation in the AuNPs-dTab solution with 100 mM NaCl solution was almost comparable to the 10 times concentrated salt solution that remains unchanged till 3 h.

room temperature. It might be due to the contamination of the solution as many synthesized samples of the AuNPs-dSol solution stored in normal conditions are randomly attacked by fungi.³⁸ To avoid this problem, we have transformed the solution phase of AuNPs-dSol into solid tablets. Also, we observed that random temperature fluctuations, humidity, and direct light interactions with the AuNPs-dSol solution might produce a purplish color with solid particles at the bottom of the vial that indicated the loss of stabilization around gold nanoparticles. This condition sharply reduced absorbance values at 520 nm, which indicated the loss of the dispersed state of AuNPs. A slightly greater decrease in the stability of the AuNPs-dSol particles as compared to AuNPs-dTab stored at room temperature is shown in Figure 5A. AuNPs-dTab remained stable under working conditions of continuous light and humidity exposure as shown in Figure 5B, while the AuNPs-Cit solution could maintain stability only for 3 h followed by a sudden decrease in stability that was approximately 30 and 65% in 4 and 5 h, respectively. Comparatively, tablets in the fridge were a little more stable than those at room temperature. It is also concluded that our fabricated tablets have shown long-term stability at room temperature under a continuous working environment to date.

The stability of particles was also measured by recording the zeta potential as particles with values greater than 20 mV or less than -20 mV have enough electrostatic repulsion to remain stable in the solution. However, it is important to note that when particles are surrounded by biopolymers, their electrostatic repulsion due to citrate ions is decreased as shown

by high ζ potential values. At this point, primarily, the stabilization force is steric in nature. The zeta potential was measured for AuNPs-Cit, AuNPs-dSol, and AuNPs-dTab solutions at pH 5.86, and values for all the samples were negative. The ζ potential obtained for the AuNPs-Cit particles was -45.4 ± 6.0 mV, while it was -6.6 ± 0.3 and -3.5 ± 0.2 mV in the case of AuNPs-dSol and AuNPs-dTab solutions, respectively. These results indicated that citrate-capped particles are more negatively charged as compared to dextran-capped particles at this pH as supported by the literature.⁶ However, the surface charge will remain identical in the case of the AuNPs-dSol solution and AuNPs-dTab. It also confirms that AuNPs-dTab is a good alternative to the AuNPs-dSol solution without any change in the stability of particles. Our fabricated tablets are free from contamination and stable for more than a year if carefully stored at a constant temperature and light.

Effect of Salt on AuNPs-dTabs. Besides the morphological properties of gold nanoparticles, surface functionality is another important aspect to be studied because functional groups attached to nanogold are directly controlling the SPR phenomenon, which is a fundamental principle of colorimetric sensors. Primary results indicated that the 100 mM NaCl solution has induced aggregation in the AuNPs-dTab solution (8.01 nM), but this aggregation is not visible to the naked eye and the solution remains red as supported by Wang *et al.*³⁵ However, UV-vis spectra showed a decrease in A_{520/650} value from 9.13 to 5.64 that confirms the aggregated state of particles. To enhance this aggregation, higher concentrations

of salt up to 1 M were tested, but there was no significant change in the visual observations as well as those by the UV–vis machine. The effect of the 100 mM salt solution was comparable to that of 1000 mM with no significant changes in the absorbance (λ_{max}) values as shown in Figure 6A. Increasing the ionic strength of the solution did not induce further destabilization in the case of AuNPs-dSol as the polysaccharide surface binding to the AuNPs provides extra stability against a higher ionic strength. However, in the case of AuNPs-Cit, as the ionic strength of the solution increased by the addition of sodium chloride, the additional ions would protect the electrostatic repulsive interactions, causing van der Waals attractive interactions to dominate and the particles to aggregate.⁵¹ Further, a kinetic study of AuNPs-dTab in the presence of 100 mM sodium chloride was performed till 3 h as shown in Figure 6B. A slight decrease in A520/650 value was observed in the inset of Figure 6B, which indicated that maximum aggregation due to salt solution happened at once and there was a negligible increase in aggregation over time.

A control experiment was carried out to check the difference between the salt concentration required to destabilize the AuNPs-Cit and AuNPs-dSol solution. Regarding 8.01 nM AuNPs, the optimum concentration of NaCl was 170 mM, which induced a good aggregation and a visible color change from red to blue. However, in the case of the AuNPs-dSol solution, stabilization forces were much stronger, and AuNPs remained dispersed/stabilized at the super saturated concentration (10 M) of NaCl. Furthermore, upon heating this solution, there was no effect in color change at all, which indicated the thermal stability of particles at high salt concentrations. This observation is also supported by the literature as Wang and co-workers³⁵ monitored the stability of the AuNPs-dSol under physiological conditions (0.157 M, NaCl) by UV–vis spectroscopy and observed that the colloidal stability is not affected at all upon the addition of a very high salt content. Further, the aggregation kinetics of dextran-capped gold nanoconjugates in the presence of 100 mM NaCl were studied to find the effect of time on the rate of aggregation. There was a negligible increase in the aggregation of particles over 3 h resulting in the spontaneous response of salt on AuNPs-dTab to promote aggregation as a quick reaction. A slight decrease in A520/650 value was observed (results are not shown here). This indicates the higher stability of dextran-capped gold nanoparticles and their higher resistance even in high ionic strength solutions. This is an important aspect that confirms the outstanding stability of dextran-capped AuNPs in the physiological saline solution so that particles can be used in analytical applications without further surface modifications.³⁵

pH-Responsive Behavior of AuNPs-dTabs. Undoubtedly, the pH responsive sensitivity of ligands attached to a gold surface has a direct influence on the optical characteristics of AuNPs. Lv *et al.* have reported that the behavior of dextran derivatives toward AuNPs is strongly pH-dependent.³¹ Stabilization around AuNPs is greatly affected by acidic or basic solutions because they can increase the dissolution rate of the nanoparticles into an ionic form that can redeposit onto existing nanoparticles, changing the average diameter and size distribution.

Initially, AuNPs-dTabs 6% (w/v) were tested against 0.1 M hydrochloric acid, 0.1 M sodium hydroxide, and 0.1 M sodium chloride solutions to see the effect of highly acidic (pH = 1.31), highly basic (pH = 13.03), and neutral (pH = 5.53)

environments on the stability of nanoparticles. Basic and ionic solutions did not induce any color change visible to the naked eye; however, the acidic condition changed the solution from red to purple color, which indicated the aggregation as shown in Figure 7A. Absorption maxima at 520 and 650 nm were

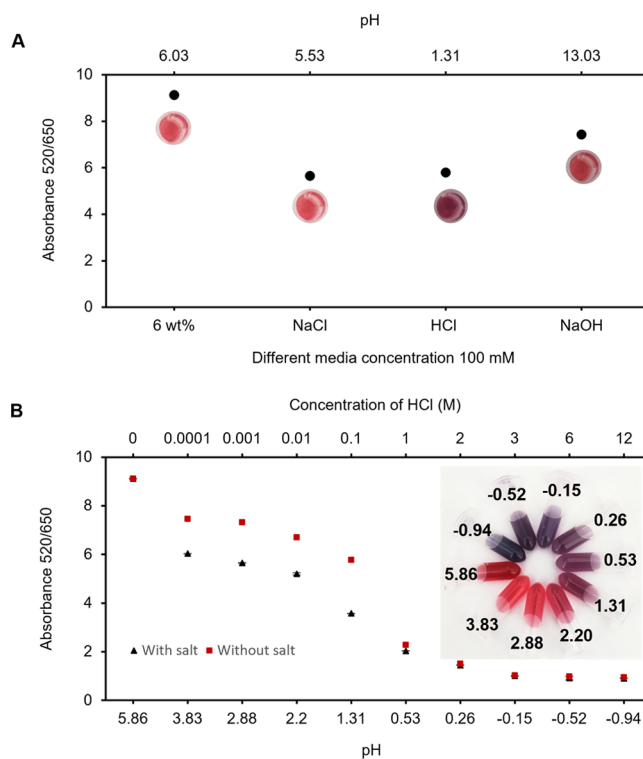


Figure 7. pH responsive behavior of AuNPs-dTab 6% (w/v). (A) Initial screening of AuNPs-dTab using 100 mM solution of sodium chloride, hydrochloric acid, and sodium hydroxide. (B) The concentration-dependent acid-promoted aggregation behavior of AuNPs-dTab with and without sodium chloride solution (100 mM) indicates the aggregation profile of AuNPs-dTab suitable for a range of applications where acid-sensitive linkages are involved. The experiment data are the mean of the three replications ($n = 3$) \pm SD where some error bars were hidden behind the data points.

recorded for all the solutions using a UV–vis spectrophotometer. Absorbance values at A520/650 nm were reduced slightly in the basic solution, whereas these values were much lower in the case of acidic conditions. This is the indication of the breaking of steric stabilization due to dextran around AuNPs that leads to the aggregation of particles. Hence, we can conclude that destabilization was prominent at a lower pH, whereas a higher pH (basic) did not cause a significant change in stabilization due to the presence of the biopolymer. Upon variation of pH, the hydrophilic–hydrophobic balance of a few polymers is disturbed by the change in the ionization state of the weak acid or base groups.³¹ The steric stabilization is the major force in this system due to dextran macromolecular configuration which is difficult to break and requires harsh conditions as compared to electrostatic stabilization of the AuNPs-Cit solution which is highly sensitive to ionic strength. In the case of AuNPs-dTab, the molecular weight of the macromolecule and surface graft density are dominant factors. In general, thicker polymer layers and higher graft densities lead to more effective steric stabilization.²⁰

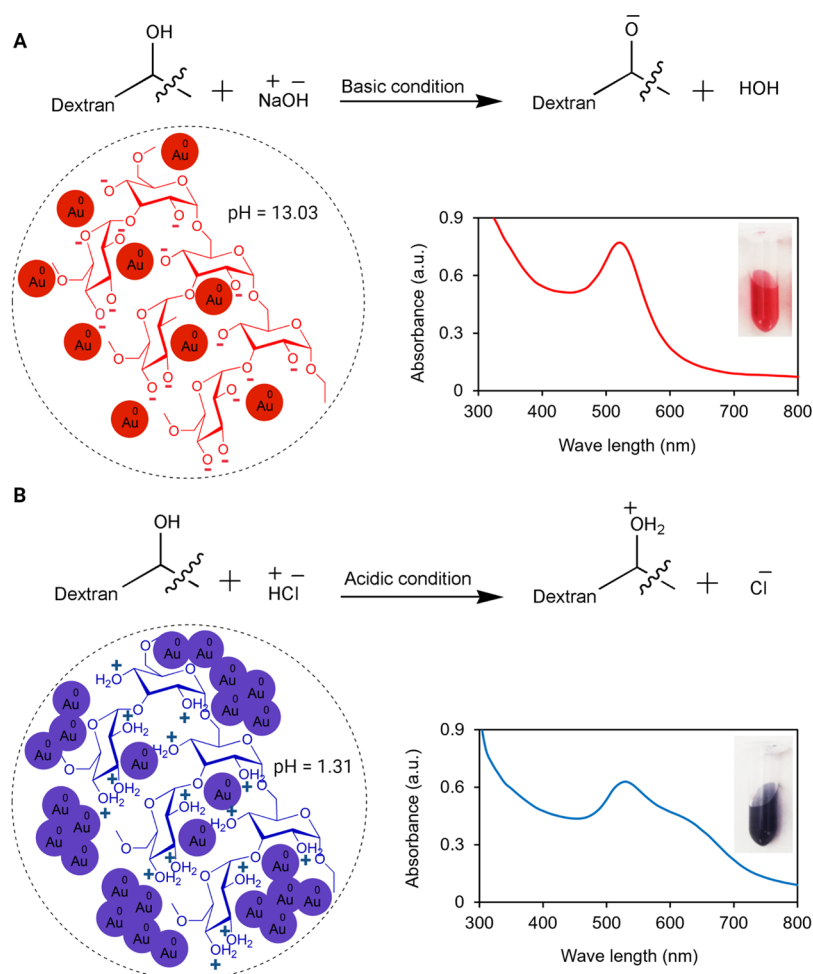


Figure 8. Influence of acidic and basic environment on AuNPs-dTab along with plausible structural drawings. (A) Particles in the AuNPs-dTab solution were stable in the alkaline condition. (B) Spontaneous acid-promoted aggregation of particles in the AuNPs-dTab solution indicating the use of AuNPs-dTab as a potential smart sensing material.

The substantial acid-catalyzed deterioration of polysaccharide molecules was investigated using AuNPs-dTab 6% (w/v) with different concentrations of hydrochloric acid ranging from 0.0001 to 12 M. Due to the abundance of hydroxyl groups in dextran, acidic pH strongly influenced the aggregation of AuNPs by protonation of $-\text{OH}$ to OH_2^+ on the dextran chain.³⁶ In the acidic condition, cations are present in the solution, and negatively charged stabilizing species around AuNPs are no longer maintained in the solution, which is why nanoparticles become destabilized and hence aggregated. This aggregation was observed by the naked eye at pH 1.31 and lower. A rapid color change happened from red to purple when 0.1 M HCl was added to the nanoparticle solution in a 1:1 ratio. However, maximum aggregation was recorded at pH 0.26, below which pH did not have any influence on color. We observed that $\text{pH} \leq 1$ induced prominent aggregation without salt due to the protonation of dextran's functional groups. The full spectra scan at 300–800 nm of AuNPs-dTab 6% (w/v) with variable hydrochloric acid concentrations in a 1:1 ratio can be seen in Figure S6. However, to improve the sensitivity of the signal, the salt solution was used in an equal ratio. As discussed previously, the effectiveness of the 100 mM NaCl solution was comparable to that of 1000 mM in this system, so the lower concentration of salt was selected. Black dots in Figure 7B represent the destabilization of the particles in the

presence of salt. It was clear that the effect of salt was predominant up to pH 1.31, and the ionic solution contributes to breaking the stabilization strongly in the presence of acid above pH 0.53. However, at pH lower than 0.53, the salt effect became negligible as maximum aggregation has already happened due to the acid aggregation of dextran.

It is well-known that dextran offers a sterically stable noncovalent coating around gold nanoparticles.^{20,52} The proposed chemical reaction along with UV-vis spectra of dispersed and aggregated dextran-capped gold nanoparticles is shown in Figure 8. The reaction media's pH greatly influences the oxygen–hydrogen bond of dextran and leave the oxygen–carbon bond intact. At pH 13.03, the electrostatic repulsive interaction between negatively charged AuNPs and negatively charged $-\text{CO}-$ of the dextran chain makes AuNPs stable, resulting in the red color of the colloidal solution as shown in Figure 8A. However, at pH 1.31, negatively charged $-\text{CO}-$ of dextran changed into $-\text{COH}$, which formed strong hydrogen bonds with each other and led to the aggregation and precipitation of AuNPs resulting in a blue solution as shown in Figure 8B.⁴⁹ This investigation also confirms the suitability of basic media for the synthesis of AuNPs-dSol. Our AuNPs-dTabs have potential applications in acid-sensitive linkages such as the hydrolysis of acetal, ketal, ester, amide, imine, hydrazone, and oxime.³² Our research is an open invitation to

researchers who are exploring the properties of nanomaterials under acidic environments such as drug delivery, tumor imaging, and diagnostic applications. For instance, at pH \sim 4, glutathione detection in human blood serum has been reported,⁵³ whereas 30 nm AuNPs-Cit have been used as an efficient pH sensor to measure the acidity.⁵⁴

CONCLUSIONS

In this research, we presented the successful formation of dextran-encapsulated AuNPs tablets (AuNPs-dTabs) by a simple and straightforward approach utilizing post-modification of AuNPs-Cit with dextran powder. These tablets provide an easy-to-use platform to have premeasured quantities of reagents for a long duration as AuNPs-dTabs were stable for at least 9 months (tablets were still stable at the time of this manuscript preparation) at room temperature and in the fridge as proven by the stability test. Once the amount inside the tablet was calibrated, there is no need of weighing and labor-intensive optimization of reagents every time. Additionally, these tablets are a low-cost (approx. 1.22 CAD per 100 tablets of 100 μ L) and easy-to-use substitute to the AuNPs-dextran solution (AuNPs-dSol) without compromising particle stability as proven by various characterization results. We have measured the tablet morphology in terms of thickness, diameter, density, and opacity using 6 and 10% dextran with 2, 4, and 8 nM AuNPs-Cit. We also reported the concentration-dependent acid-promoted aggregation of tablets at variable pH that can be seen by the naked eye due to the strong colorimetric response of nanoparticles from red to blue. However, neutral and basic conditions favor the stability of tablets and render the particles well-dispersed in the colloidal solution. We believe that the AuNPs-dTabs presented in this study have a great potential to be used in colorimetric detection applications where acid-sensitive aggregation is the primary concern. This smart material shows a promising potential for future applications in nanosensing and diagnostics. Hence, researchers could pay attention to explore these tablets to prepare ready-to-use kits for the detection of hazardous analytes of interest for environmental monitoring and food assessment. Moreover, further investigation is required to apply an encapsulation strategy toward functionalized AuNPs and to understand the variable factors affecting the steric stabilization of the polymer around AuNPs in a tablet platform.

EXPERIMENTAL SECTION

Materials and Methods. All reagents and solvents were used as received without further purification. Gold(III) chloride solution 99.99% (trace metals basis, 30 wt % in dilute HCl) and trisodium citrate dihydrate were purchased from Sigma Aldrich, USA. HPLC-grade water, hydrochloric acid 37%, and nitric acid 65% were purchased from Sigma Aldrich. Dextran (*Leuconostoc* spp., $M \sim$ 100 kDa) was purchased from Sigma Aldrich, China. Sodium hydroxide was purchased from Sigma Aldrich, Switzerland. Sodium chloride was purchased from the central chemical store of Concordia University. The plastic sheet of polypropylene was purchased from a local stationary shop.

pH measurements were recorded using plastic pH indicator strips made by Fisher Scientific, USA, and an accumetAB200 pH/mV/conductivity meter made by Fisher Scientific, Singapore. The *ImageJ* software from the National Institutes

of Health, Bethesda, MD, USA, was used. A vortex (model # 9454FIALUS, 50/60 Hz Fisherbrand) was used to get a homogenized AuNPs-dTab solution. A particle size analyzer (PSA) (model Litesizer 500, Anton-Paar, Austria) was used for nanoparticle size distribution and polydispersity index. The particle size range for the machine is 0.3 nm–10 μ m. All samples were also run for zeta potential *via* electrophoretic light scattering using the cmPALS technique (European Patent 2735870) for high sensitivity. PSA has a particle size range from 3.8 nm to 100 μ m for zeta potential measurements. The colloidal concentration of nanoparticles was taken in Ω -shaped polystyrene cuvettes at 25 $^{\circ}$ C, and the data were taken in triplicate.

The extinction spectra of AuNPs were recorded on a UV–vis spectrophotometer (BioTek, Cytation 5, imaging reader) at room temperature. Infrared spectra of samples were obtained from a Nicolet iS20 FTIR spectrometer (Thermo Scientific Instrument Co., Madison, Wisconsin, USA) using the single reflection horizontal ATR accessory Smart Orbit and a diamond crystal with ZnSe lens at an incident angle of 42 $^{\circ}$. The FTIR spectra were acquired in the range of 4200 to 650 cm^{-1} with a 0.25 cm^{-1} spectral resolution to identify potential chemical interactions between dextran and gold nanoparticles. Each sample was scanned twice to ensure good reproducibility. Transmission electron microscopy (TEM) was performed using a Talos L120C (20–120 kV) for structural examinations and investigation of particle shape and size. We used a copper grid with a coating of formvar (FCF-300-CU, 300 mesh) purchased from Electron Microscopy Sciences. AuNP solutions (2 μ L) were deposited on a grid and dried for 24 h before performing the run.

The surface morphology measurement and data acquisition of the AuNPs-dTab sample were carried out by an atomic force microscopy (AFM) system (Anton Paar Tosca 400, Austria) with the tapping mode in air. An aluminum reflex coated cantilever (thickness: 30 nm, resonance frequency: 285 kHz, spring constants: 42 Nm^{-1} , curvature radius: <10 nm, and height 10–15 μ m) was used for the experiment, and the 500 \times 500 pixel images were collected at a line rate of 1 lines/s. Image analysis was done using Gwyddion (free, open-source software, version 2.59).

Formation of the Dextran-Capped Gold Nanoparticle Solution. In the first step, citrate-capped gold nanoparticles (AuNPs-Cit) were prepared following the direct method of the Turkevich approach⁴² with slight modifications. The concentration of this colloidal solution was estimated to be 8.01 nM according to Beer's law while using an extinction coefficient (ϵ) of 13 nm AuNPs due to their surface plasmon resonance (SPR) wavelength at 520 nm.⁴² In the second step, dextran-capped gold nanoparticles (AuNPs-dSol) were achieved by replacing citrate ions with dextran being the strong stabilizer as well as capping agent. This is called "post-modification of preformed AuNPs". For this purpose, the concentration of polysaccharide solution in weight by volume (w/v) was used to cast the tablets where 10 g of dextran powder was mixed using the vortex with the required volume of AuNPs-Cit suspension to get the 10% (w/v) solution of AuNPs-dSol. From this stock solution, serial dilutions of 1–9% (w/v) AuNPs-dSol were prepared for further experiments. FTIR spectra of AuNPs-Cit and AuNPs-dSol samples were recorded to identify the functional groups around gold nanoparticles and their surface chemistry.

Formation of Dextran-Capped Gold Nanoparticles Tablets (AuNPs-dTabs) and Their Morphological Studies. AuNPs-dTabs were casted by squeeze dropping 100 μL of the AuNPs-dSol solution of variable % concentrations (w/v) on a clean plastic sheet of polypropylene. The drops were air-dried overnight at 20 $^{\circ}\text{C}$, 48% RH, and atmospheric pressure. In another batch, tablets were dried in an oven at 80 $^{\circ}\text{C}$ to compare the effect of heat on tablet formation. Tablet formation was considered not fully completed if the tablet could not be removed from the sheet. The uniformity and color of all tablets (1–10% (w/v)) were recorded. These tablets were dissolved in a fixed volume of water to observe the dispersion of colloidal nanoparticles in the solution by recording the absorbance at 520 and 650 nm UV–vis spectrophotometrically.

Once the optimum ratio of dextran and AuNPs-Cit solution was obtained depending upon the stability of particles, tablets of variable sizes such as 50, 100, 200, 300, 400, and 500 μL were casted to see the effect of volume on the tablets' diameter. To study further, 100 μL of different concentration of AuNPs (8, 4, and 2 nM) was mixed with different amounts of dextran separately to get 6 and 10% (w/v) tablets. These tablets were considered for measuring the hydrodynamic diameter (ϕ , mm), thickness (e , mm), density (ρ , g/cm^3), and opacity (Op , A/mm).

The particle size and shape were recorded through TEM analysis, and AuNPs-dTab was compared with the AuNPs-Cit solution. The topological network of gold nanoparticles embedded in the dextran matrix has been successfully imaged by AFM in the tapping mode. This nano-imaging with high spatial resolution and exceptionally low invasiveness is useful to explain the particle height. The line profiles were used to determine the height and length for each particle. Moreover, for the crystallinity and thermal analysis of the AuNPs-dTab material, XRD and DSC studies were carried out.

Stability of AuNPs-dTabs. The stability of AuNPs-dTabs placed in different conditions was determined by measuring the absorbance at 520 nm on different days. These tablets were kept at 20 and 4 $^{\circ}\text{C}$ for different lengths of time such as 1, 7, 14, 21, 28, 90, 180, and 270 days before being tested. These tablets were also stored in open air and air-tight packing to study the effect of humidity on the performance of AuNPs-dTabs. To test the dispersion state of nanoparticles, 200 μL of HPLC water was used to dissolve two AuNPs-dTabs (100 μL , 5.79 mm diameter \times 0.313 mm thickness) to obtain a homogeneous solution and then transferred to a 96-well plate to measure the absorbance of red color. The observation was recorded in triplicate at 520 nm on a UV–vis spectrophotometer plate reader and compared with the AuNPs-dSol solution. To ensure the stability of rest of the tablets/solution over the period of time, only an aliquot was taken out for the measurement each time. A comparative stability study was also conducted between the AuNPs-dTab and AuNPs-Cit solution under working environmental conditions where both the samples were exposed to ambient temperature and light continuously. Zeta potential and dynamic light scattering studies were also conducted to see the stability of different colloidal solutions such as the AuNPs-Cit, AuNPs-dSol, and AuNPs-dTab solution.

Screening of AuNPs-dTabs under Variable Ionic Strengths and pHs. The effect of different concentrations of sodium chloride (100–1000 mM) on the aggregation behavior of AuNPs was studied using 6% AuNPs-dTab.

Different strengths of acidic and alkaline media were also provided to the AuNPs-dTab to check the pH-responsive behavior as well as sensitivity of the tablet material. For this purpose, these tablets were dissolved in a required amount of HPLC-grade water using a vortex to get a homogenized colloidal dispersion. Subsequently, 0.1 M NaCl, 0.1 M HCl, and 0.1 M NaOH solutions were added in separate vials in a 1:1 ratio with the AuNPs-dTab solution. The absorbance of the solution at 520 and 650 nm was recorded using a UV–vis spectrophotometer. Based on this initial screening, the dextran-stabilized AuNP aggregation assay was optimized at variable pHs in the acidic range. The kinetic study of AuNPs-dTab 6% (w/v) was performed with 0.1 M NaCl concentration till 3 h. Finally, a comparative analysis of the acid-induced aggregation of AuNPs-dTab solution was conducted in the presence and absence of 100 mM sodium chloride solution.

Statistical Analysis. All statistical analyses were performed by Microsoft Excel 2019. The unpaired Student t test was used to identify the statistically significant differences between the results, with p values < 0.05 interpreted as significant.

■ ASSOCIATED CONTENT

Supporting Information

The Supporting Information is available free of charge at <https://pubs.acs.org/doi/10.1021/acsomega.1c07393>.

List of abbreviations as well as additional experimental details to record tablet physical characteristics, materials for XRD and DSC analysis, results including supplemental Figures S1–S6 depicting photographs of AuNPs-dTab, XRD and DSC spectra, AFM images of 2D and 3D of height trace, and UV–vis spectra (300–800 nm) of acid-induced aggregation of AuNPs-dTab (PDF)

■ AUTHOR INFORMATION

Corresponding Author

Sana Jahanshahi-Anbuhi – Department of Chemical and Materials Engineering, Gina Cody School of Engineering, Concordia University, Montréal, Québec H4B 1R6, Canada; orcid.org/0000-0002-2191-8430; Email: sana.anbuhi@concordia.ca

Authors

Zubi Sadiq – Department of Chemical and Materials Engineering, Gina Cody School of Engineering, Concordia University, Montréal, Québec H4B 1R6, Canada

Seyed Hamid Safiabadi Tali – Department of Chemical and Materials Engineering, Gina Cody School of Engineering, Concordia University, Montréal, Québec H4B 1R6, Canada

Complete contact information is available at: <https://pubs.acs.org/10.1021/acsomega.1c07393>

Notes

The authors declare no competing financial interest.

■ ACKNOWLEDGMENTS

The authors acknowledge the Natural Sciences and Engineering Research Council of Canada (NSERC) for funding this work through a Discovery Grant and the Concordia University for the Concordia University Research Chair (CURC) fund for development of Stable Bio/Chemosensors. The authors also thank the Centre for NanoScience Research (CeNSR) funded by Concordia University, Montreal, Canada, for their

assistance in capturing the TEM images. Many thanks to Prof. Zhibin Ye and Ms. Bahareh Raisi from the Polymer & Nanomaterials laboratory for supporting with the XRD study and laboratory technician Kerri Warbanski for assisting with running the FTIR, DLS, AFM, and DSC analysis.

REFERENCES

- (1) Sankar, M.; He, Q.; Engel, R. V.; Sainna, M. A.; Logsdail, A. J.; Roldan, A.; Willock, D. J.; Agarwal, N.; Kiely, C. J.; Hutchings, G. J. Role of the Support in Gold-Containing Nanoparticles as Heterogeneous Catalysts. *Chem. Rev.* **2020**, *120*, 3890–3938.
- (2) dos Santos, C. A.; Ingle, A. P.; Rai, M. The Emerging Role of Metallic Nanoparticles in Food. *Appl. Microbiol. Biotechnol.* **2020**, *104*, 2373–2383.
- (3) Phummirat, P.; Mann, N.; Preece, D.; Preece, D. Applications of Optically Controlled Gold Nanostructures in Biomedical Engineering. *Front. Bioeng. Biotechnol.* **2021**, *8*, 1472.
- (4) Bansal, S. A.; Kumar, V.; Karimi, J.; Singh, A. P.; Kumar, S. Role of Gold Nanoparticles in Advanced Biomedical Applications. *Nanoscale Adv.* **2020**, *2*, 3764–3787.
- (5) Nejati, K.; Dadashpour, M.; Gharibi, T.; Mellatyar, H.; Akbarzadeh, A. Biomedical Applications of Functionalized Gold Nanoparticles: A Review. *J. Cluster Sci.* **2021**, 1–16.
- (6) Lee, K.-C.; Chen, W.-J.; Chen, Y.-C. Using Dextran-Encapsulated Gold Nanoparticles as Insulin Carriers to Prolong Insulin Activity. *Nanomedicine* **2017**, *12*, 1823–1834.
- (7) Wang, F.; Wang, Y. C.; Dou, S.; Xiong, M. H.; Sun, T. M.; Wang, J. Doxorubicin-Tethered Responsive Gold Nanoparticles Facilitate Intracellular Drug Delivery for Overcoming Multidrug Resistance in Cancer Cells. *ACS Nano* **2011**, *5*, 3679–3692.
- (8) Retout, M.; Blond, P.; Jabin, I.; Bruylants, G. Ultrastable PEGylated Calixarene-Coated Gold Nanoparticles with a Tunable Bioconjugation Density for Biosensing Applications. *Bioconjugate Chem.* **2021**, *32*, 290–300.
- (9) Yu, Y.; Su, G.; Zhang, W. S.; Pan, J.; Li, F.; Zhu, M.; Xu, M.; Zhu, H. Reverse Transcription Recombinase Polymerase Amplification Coupled with CRISPR-Cas12a for Facile and Highly Sensitive Colorimetric SARS-CoV-2 Detection. *Anal. Chem.* **2021**, *93*, 4126–4133.
- (10) Hu, S.; Huang, P.-J. J.; Wang, J.; Liu, J. Dissecting the Effect of Salt for More Sensitive Label-Free Colorimetric Detection of DNA Using Gold Nanoparticles. *Anal. Chem.* **2020**, *92*, 13354–13360.
- (11) Pinheiro, T.; Marques, A. C.; Carvalho, P.; Martins, R.; Fortunato, E. Paper Microfluidics and Tailored Gold Nanoparticles for Nonenzymatic, Colorimetric Multiplex Biomarker Detection. *ACS Appl. Mater. Interfaces* **2021**, *13*, 3576–3590.
- (12) Si, P.; Razmi, N.; Nur, O.; Solanki, S.; Pandey, C. M.; Gupta, R. K.; Malhotra, B. D.; Willander, M.; de la Zerda, A. Gold Nanomaterials for Optical Biosensing and Bioimaging. *Nanoscale Adv.* **2021**, *3*, 2679–2698.
- (13) Kalimuthu, K.; Cha, B. S.; Kim, S.; Park, K. S. Eco-Friendly Synthesis and Biomedical Applications of Gold Nanoparticles: A Review. *Microchem. J.* **2020**, *152*, 104296.
- (14) Wuithschick, M.; Birnbaum, A.; Witte, S.; Sztucki, M.; Vainio, U.; Pinna, N.; Rademann, K.; Emmerling, F.; Kraehnert, R.; Polte, J. Turkevich in New Robes: Key Questions Answered for the Most Common Gold Nanoparticle Synthesis. *ACS Nano* **2015**, *9*, 7052–7071.
- (15) Schulz, F.; Homolka, T.; Bastús, N. G.; Puntès, V.; Weller, H.; Vossmeier, T. Little Adjustments Significantly Improve the Turkevich Synthesis of Gold Nanoparticles. *Langmuir* **2014**, *30*, 10779–10784.
- (16) Liu, H.; Ikeda, K.; Nguyen, M. T.; Sato, S.; Matsuda, N.; Tsukamoto, H.; Tokunaga, T.; Yonezawa, T. Alginate-Stabilized Gold Nanoparticles Prepared Using the Microwave-Induced Plasma-in-Liquid Process with Long-Term Storage Stability for Potential Biomedical Applications. *ACS Omega* **2022**, 1c06769.
- (17) Sarfraz, N.; Khan, I. Plasmonic Gold Nanoparticles (AuNPs): Properties, Synthesis and Their Advanced Energy, Environmental and Biomedical Applications. *Chem. - Asian J.* **2021**, *16*, 720–742.
- (18) Chowdhury, S.; Teoh, Y. L.; Ong, K. M.; Raffliaman Zaidi, N. S.; Mah, S.-K. Poly(Vinyl Alcohol Crosslinked Composite Packaging Film Containing Gold Nanoparticles on Shelf Life Extension of Banana. *Food Packag. Shelf-Life* **2020**, *24*, 100463.
- (19) Sarpong, K. A.; Zhang, K.; Luan, Y.; Cao, Y.; Xu, W. Development and Application of a Novel Electrochemical Sensor Based on AuNPs and Difunctional Monomer-MIPs for the Selective Determination of Tetrabromobisphenol-S in Water Samples. *Microchem. J.* **2020**, *154*, 104526.
- (20) Zhao, W.; Brook, M. A.; Li, Y. Design of Gold Nanoparticle-Based Colorimetric Biosensing Assays. *ChemBioChem* **2008**, *9*, 2363–2371.
- (21) Hua, Z.; Yu, T.; Liu, D.; Xianyu, Y. Recent Advances in Gold Nanoparticles-Based Biosensors for Food Safety Detection. *Biosens. Bioelectron.* **2021**, *179*, 113076.
- (22) Priyadarshini, E.; Pradhan, N. Gold Nanoparticles as Efficient Sensors in Colorimetric Detection of Toxic Metal Ions: A Review. *Sens. Actuators, B* **2017**, *238*, 888–902.
- (23) Zhang, W.; Wang, Y.; Nan, M.; Li, Y.; Yun, J.; Wang, Y.; Bi, Y. Novel Colorimetric Aptasensor Based on Unmodified Gold Nanoparticle and SsDNA for Rapid and Sensitive Detection of T-2 Toxin. *Food Chem.* **2021**, *348*, 129128.
- (24) Kasoju, A.; Shrikrishna, N. S.; Shahdeo, D.; Khan, A. A.; Alanazi, A. M.; Gandhi, S. Microfluidic Paper Device for Rapid Detection of Aflatoxin B1 Using an Aptamer Based Colorimetric Assay. *RSC Adv.* **2020**, *10*, 11843–11850.
- (25) Kasoju, A.; Shahdeo, D.; Khan, A. A.; Shrikrishna, N. S.; Mahari, S.; Alanazi, A. M.; Bhat, M. A.; Giri, J.; Gandhi, S. Fabrication of Microfluidic Device for Aflatoxin M1 Detection in Milk Samples with Specific Aptamers. *Sci. Rep.* **2020**, *10*, 4627.
- (26) Zahra, Q. u. A.; Luo, Z.; Ali, R.; Khan, M. I.; Li, F.; Qiu, B. Advances in Gold Nanoparticles-Based Colorimetric Aptasensors for the Detection of Antibiotics: An Overview of the Past Decade. *Nanomaterials* **2021**, *11*, 840.
- (27) Zha, Y.; Lu, S.; Hu, P.; Ren, H.; Liu, Z.; Gao, W.; Zhao, C.; Li, Y.; Zhou, Y. Dual-Modal Immunosensor with Functionalized Gold Nanoparticles for Ultrasensitive Detection of Chloroacetamide Herbicides. *ACS Appl. Mater. Interfaces* **2021**, *13*, 6091–6098.
- (28) Shrivastava, P.; Singh, B. P.; Jain, S. K.; Jain, V. K.; Nagpal, S. A Novel Approach to Detect Barium in Gunshot Residue Using a Handheld Device: A Forensic Application. *Anal. Methods* **2021**, *13*, 4379–4389.
- (29) Jang, H.; Ryoo, S.; Kostarelos, K.; Woo, S.; Min, D. Biomaterials The Effective Nuclear Delivery of Doxorubicin from Dextran-Coated Gold Nanoparticles Larger than Nuclear Pores. *Biomaterials* **2013**, *34*, 3503–3510.
- (30) Safiabadi Tali, S. H.; LeBlanc, J. J.; Sadiq, Z.; Oyewunmi, O. D.; Camargo, C.; Nikpour, B.; Armanfard, N.; Sagan, S. M.; Jahanshahi-Anbuhi, S. Tools and Techniques for Severe Acute Respiratory Syndrome Coronavirus 2 (SARS-CoV-2)/COVID-19 Detection. *Clin. Microbiol. Rev.* **2021**, *34*, No. e00228-20.
- (31) Lv, W.; Liu, S.; Fan, X.; Wang, S.; Zhang, G.; Zhang, F. Gold Nanoparticles Functionalized by a Dextran-Based PH- And Temperature-Sensitive Polymer. *Macromol. Rapid Commun.* **2010**, *31*, 454–458.
- (32) Jazani, A. M.; Oh, J. K. Development and Disassembly of Single and Multiple Acid-Cleavable Block Copolymer Nanoassemblies for Drug Delivery. *Polym. Chem.* **2020**, *11*, 2934–2954.
- (33) Zhang, Y.; Yang, L.; Yang, C.; Liu, J. Recent Advances of Smart Acid-responsive Gold Nanoparticles in Tumor Therapy. *Wiley Interdiscip. Rev.: Nanomed. Nanobiotechnol.* **2020**, *12*, No. e1619.
- (34) Chen, F.; Huang, G.; Huang, H. Preparation and Application of Dextran and Its Derivatives as Carriers. *Int. J. Biol. Macromol.* **2020**, *145*, 827–834.
- (35) Wang, Y.; Zhan, L.; Huang, C. Z. One-Pot Preparation of Dextran-Capped Gold Nanoparticles at Room Temperature and

Colorimetric Detection of Dihydralazine Sulfate in Uric Samples. *Anal. Methods* **2010**, *2*, 1982–1988.

(36) Davidović, S.; Lazić, V.; Vukoje, I.; Papan, J.; Anhrenkiel, S. P.; Dimitrijević, S.; Nedeljković, J. M. Dextran Coated Silver Nanoparticles — Chemical Sensor for Selective Cysteine Detection. *Colloids Surf., B* **2017**, *160*, 184–191.

(37) Prusty, K.; Swain, S. K. Nanostructured Gold Dispersed Polyethylmethacrylate / Dextran Hybrid Composites for Packaging Applications. *Polym.-Plast. Technol. Mater.* **2019**, *58*, 2019–2030.

(38) Diem, P. H. N.; Thao, D. T. T.; Van Phu, D.; Duy, N. N.; Quy, H. T. D.; Hoa, T. T.; Hien, N. Q. Synthesis of Gold Nanoparticles Stabilized in Dextran Solution by Gamma Co-60 Ray Irradiation and Preparation of Gold Nanoparticles/Dextran Powder. *J. Chem.* **2017**, *2017*, 6836375.

(39) Cai, H.; Yao, P. In Situ Preparation of Gold Nanoparticle-Loaded Lysozyme-Dextran Nanogels and Applications for Cell Imaging and Drug Delivery. *Nanoscale* **2013**, *5*, 2892–2900.

(40) Xia, C.; Ren, B.; Liu, N.; Zheng, Y. A Feasible Strategy of Fabricating of Gold-Encapsulated Dextran/Polyvinyl Alcohol Nanoparticles for the Treatment and Care of Wound Healing. *J. Cluster Sci.* **2021**, 1–9.

(41) Nath, S.; Kaittanis, C.; Tinkham, A.; Perez, J. M. Dextran-Coated Gold Nanoparticles for the Assessment of Antimicrobial Susceptibility. *Anal. Chem.* **2008**, *80*, 1033–1038.

(42) Esfahani, A. R.; Sadiq, Z.; Oyewunmi, O. D.; Safiabadi Tali, S. H.; Usen, N.; Boffito, D. C. C.; Jahanshahi-Anbuhi, S.; Safiabadi-Tali, S. H.; Usen, N.; Boffito, D. C. C.; Jahanshahi-Anbuhi, S. Portable, Stable, and Sensitive Assay to Detect Phosphate in Water with Gold Nanoparticles (AuNPs) and Dextran Tablet. *Analyst* **2021**, *146*, 3697–3708.

(43) Jahanshahi-Anbuhi, S.; Pennings, K.; Leung, V.; Liu, M.; Carrasquilla, C.; Kannan, B.; Li, Y.; Pelton, R.; Brennan, J. D.; Filipe, C. D. M. Pullulan Encapsulation of Labile Biomolecules to Give Stable Bioassay Tablets. *Angew. Chem., Int. Ed.* **2014**, *53*, 6155–6158.

(44) Oyewunmi, O. D.; Safiabadi-Tali, S. H.; Jahanshahi-Anbuhi, S. Dual-Modal Assay Kit for the Qualitative and Quantitative Determination of the Total Water Hardness Using a Permanent Marker Fabricated Microfluidic Paper-Based Analytical Device. *Chemosensors* **2020**, *8*, 97.

(45) Kettemann, F.; Birnbaum, A.; Witte, S.; Wuthschick, M.; Pinna, N.; Kraehnert, R.; Rademann, K.; Polte, J. Missing Piece of the Mechanism of the Turkevich Method: The Critical Role of Citrate Protonation. *Chem. Mater.* **2016**, *28*, 4072–4081.

(46) Tang, J.; Fu, X.; Ou, Q.; Gao, K.; Man, S.; Guo, J.; Liu, Y. Hydroxide Assisted Synthesis of Monodisperse and Biocompatible Gold Nanoparticles with Dextran. *Mater. Sci. Eng., C* **2018**, *93*, 759–767.

(47) Nur, H.; Nasir, S. M. Gold Nanoparticles Embedded on the Surface of Polyvinyl Alcohol Layer. *J. Fundam. Sci.* **2014**, *4* (), DOI: 10.11113/mjfas.v4n1.33.

(48) Tripathy, P.; Mishra, A.; Ram, S.; Fecht, H. J.; Bansmann, J.; Behm, R. J. X-Ray Photoelectron Spectrum in Surface Interfacing of Gold Nanoparticles with Polymer Molecules in a Hybrid Nanocomposite Structure. *Nanotechnology* **2009**, *20*, No. 075701.

(49) Huang, L.; Zhai, M.; Peng, J.; Xu, L.; Li, J.; Wei, G. Synthesis, Size Control and Fluorescence Studies of Gold Nanoparticles in Carboxymethylated Chitosan Aqueous Solutions. *J. Colloid Interface Sci.* **2007**, *316*, 398–404.

(50) Sung, A.; Piirma, I. Electrosteric Stabilization of Polymer Colloids. *Langmuir* **1994**, *1*, 1393–1398.

(51) Chiu, R. Y. T.; Nguyen, P. T.; Wang, J.; Jue, E.; Wu, B. M.; Kamei, D. T. Dextran-Coated Gold Nanoparticles for the Concentration and Detection of Protein Biomarkers. *Ann. Biomed. Eng.* **2014**, *42*, 2322–2332.

(52) Schubert, J.; Chanana, M. Coating Matters: Review on Colloidal Stability of Nanoparticles with Biocompatible Coatings in Biological Media, Living Cells and Organisms. *Curr. Med. Chem.* **2018**, *25*, 4553–4586.

(53) Kumar, V.; Bano, D.; Singh, D. K.; Mohan, S.; Singh, V. K.; Hasan, S. H. Size-Dependent Synthesis of Gold Nanoparticles and Their Peroxidase-like Activity for the Colorimetric Detection of Glutathione from Human Blood Serum. *ACS Sustainable Chem. Eng.* **2018**, *6*, 7662–7675.

(54) Abdul-Ameer, Z. N. Novelty Au Nanoparticles with Different Nano Sizes as an Acidity Sensor. *Rev. Compos. Mater. Av.* **2021**, *31*, 169–173.